Scanning Tunneling Microscopy of Dimeric and Polymeric Products of Electroreduced [Re(CO)$_3$(4-vinyl,4′-methyl-2,2′-bipyridine)Cl]

Shelly R. Snyder,[†] Henry S. White,*[,†] Silvia López,[‡] and Héctor D. Abruña*[,‡]

Contribution from the Department of Chemical Engineering and Materials Science, University of Minnesota, Minneapolis, Minnesota 55455, and Department of Chemistry, Baker Laboratory, Cornell University, Ithaca, New York 14853. *Received August 10, 1989*

Abstract: Scanning tunneling microscopy (STM) was used to image adsorbed products resulting from electroreduction of [Re(CO)$_3$(vbpy)Cl] (vbpy = 4-vinyl,4′-methyl-2,2′-bipyridine) on highly oriented pyrolytic graphite (HOPG). STM images, in air, of HOPG electrodes following electroreduction of [Re(CO)$_3$(vbpy)Cl] (in acetonitrile/0.1 M tetra-*n*-butylammonium perchlorate) by cycling the potential between 0 and −2.0 V vs a sodium saturated calomel electrode (SSCE) show molecular species uniformly distributed on the surface including approximately "dumbbell" shaped molecules (~40 × 20 Å). The size and shape of these aggregates is consistent with products derived from vinyl–vinyl coupling of Re–Re bonded dimers: [(vbpy)(CO)$_3$Re–Re(CO)$_3$(vbpyH–vbpyH)(CO)$_3$Re–Re(CO)$_3$(vbpy)]. STM images of electrodes prepared by cycling the potential between 0 and −1.45 V vs SSCE (less reducing conditions) show highly nonuniform coating of the surface by polymer. Several polymer morphologies were observed with polymer nucleation preferentially occurring at step sites on HOPG.

We describe scanning tunneling microscopy (STM) of adsorbed products resulting from electroreduction of [Re(CO)$_3$(4-vinyl-,4′-methyl-2,2′-bipyridine)Cl] (abbreviated hereinafter as [Re(CO)$_3$(vbpy)Cl] and whose structure (fac isomer) is shown below) on highly oriented pyrolytic graphite electrodes (HOPG). Electroreduction of [Re(CO)$_3$(vbpy)Cl] in acetonitrile yields a

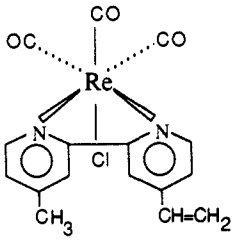

stable, electrochemically active polymer film that is capable of electrocatalytic and photoelectrocatalytic reduction of CO_2 to CO on metallic and semiconductor electrodes.[1] The synthesis and properties of polymers based on [Re(CO)$_3$(vbpy)Cl] and similar complexes have been extensively studied[1-3] by using electrochemical and spectroscopic techniques.

The chemical composition of thin films resulting from reductive polymerization of [Re(CO)$_3$(vbpy)Cl] at metal electrodes has previously been shown to depend on the experimental conditions at which reduction is performed.[1] Voltammetric studies indicate that the initial 1e$^-$ reduction of [Re(CO)$_3$(vbpy)Cl] at −1.45 V vs SSCE (sodium saturated calomel reference electrode) yields the corresponding radical anion that polymerizes through chemistry associated with the vinyl substituent on the vbpy ligand. Mechanistic details of this polymerization are not documented; however, in analogous reactions involving [ML$_2$(vbpy)]$^{2+}$, where M = Fe or Ru and L = bipyridine or phenanthroline, experimental evidence supports reductive polymerization occurring either by (a) chain propagation via linear vinyl–vinyl coupling[2,3] or (b) radical–radical coupling between the vinyl substituent and a carbon atom of L.[4]

In addition to polymerization, slow loss of Cl$^-$ from the electrogenerated radical anion accompanied by Re–Re bond formation has been unequivocally demonstrated.[5] Depending on the potential range scanned and the scan rate employed in the electrodeposition (vide infra), polymer films can be formed that are either predominantly polymerized monomer (bright yellow films) or mixtures of the monomer and dimer (greenish-yellow films).

The extent to which the Re–Re dimer is present in the polymer films can be ascertained by coulometric analysis and UV–vis spectroscopy. However, the molecular structure of polymer films containing either monomer and/or Re–Re dimer is essentially unknown. Inclusion of the dimeric species within the polymer film can be envisioned to lead to a number of structures; in particular, enhanced branching and cross-linking of polymer chains would be expected in films that contain a small fraction of dimer.

We report ex situ STM results showing polymer and adsorbed molecules deposited on the surface of HOPG electrodes following electroreduction of [Re(CO)$_3$(vbpy)Cl]. In situ and ex situ STM have been recently employed in electrochemical investigations concerning electrode topography,[6,7] oxide and metal film growth,[8,9] polypyrrole films,[10] and the deposition of ad-atoms on single crystals.[11,12] In addition, molecularly resolved images of copper–phthalocyanine adsorbed on a copper single crystal under ultrahigh vacuum conditions have been recently reported.[13] To our knowledge, however, the results reported herein represent the first images of an organometallic complex deposited by electrochemical techniques.

* Authors to whom correspondence should be addressed.
† University of Minnesota.
‡ Cornell University.

(1) (a) O'Toole, T. R.; Margerum, L. D.; Westmoreland, T. D.; Vining, W. J.; Murray, R. W.; Meyer, T. J. *J. Chem. Soc., Chem. Commun.* **1985**, 1416. (b) Cabrera, C. R.; Abruña, H. D. *J. Electroanal. Chem.* **1986**, *209*, 101.
(2) (a) Denisevich, P.; Abruña, H. D.; Leidner, C. R.; Meyer, T. J.; Murray, R. W. *Inorg. Chem.* **1982**, *21*, 2153. (b) Calvert, J. M.; Schmehl, R. H.; Sullivan, B. P.; Facci, J. S.; Meyer, T. J.; Murray, R. W. *Inorg. Chem.* **1983**, *22*, 2151.
(3) Abruña, H. D. *Coord. Chem. Rev.* **1988**, *86*, 135.
(4) Guarr, T. F.; Anson, F. C. *J. Phys. Chem.* **1987**, *91*, 4037.
(5) (a) Breikss, A. I.; Abruña, H. D. *J. Electroanal. Chem.* **1986**, *201*, 347. (b) Sullivan, B. P.; Bolinger, C. M.; Conrad, D.; Vining, W. J.; Meyer, T. J. *J. Chem. Soc., Chem. Commun.* **1985**, 1414. (c) Hawecker, J.; Lehn, J.-M.; Ziessel, R. *Helv. Chim. Acta* **1986**, *69*, 1990. (d) O'Toole, T. R.; Sullivan, B. P.; Bruce, M. R.-M.; Margerum, L. D.; Murray, R. W.; Meyer, T. J. *J. Electroanal. Chem.* **1989**, *259*, 217.
(6) Fan, F. F.; Bard, A. J. *Anal. Chem.* **1988**, *60*, 751.
(7) (a) Wiechers, J.; Twomey, T.; Kolb, D. M.; Behm, R. J. *J. Electroanal. Chem.* **1988**, *248*, 451. (b) Vazquez, L.; Rodriquez, J. M.; Herrero, J.; Baro, A. M.; Garcia, N.; Canullo, J. C.; Arvia, A. J. *Surf. Sci.* **1987**, *181*, 98. (c) Vazquez, L.; Bartolome, A.; Baro, A. M.; Alonso, C.; Savarezza, R. C.; Arvia, A. J. *Surf. Sci.* **1989**, *215*, 171.
(8) Gerwirth, A. A.; Bard, A. J. *J. Phys. Chem.* **1988**, *92*, 5563.
(9) Scott, E.; White, H. S. *J. Phys. Chem.* **1989**, *93*, 5249.
(10) Yang, R.; Dalsin, K. M.; Evans, F.; Christensen, L.; Hendrickson, W. A. *J. Phys. Chem.* **1989**, *93*, 511.
(11) Schardt, B. C.; Yau, S.; Rinaldi, F. *Science* **1989**, *243*, 1050.
(12) Marchon, B.; Bernhardt, P.; Bussell, M. E.; Somorjai, G. A.; Salmeron, M.; Siekhaus, W. *Phys. Rev. Lett.* **1988**, *60*(*12*), 1166.
(13) Lippel, P. H.; Wilson, R. J.; Miller, M. D.; Woll, C. H.; Chiang, S. *Phys. Rev. Lett.* **1989**, *62*(*2*), 171.

0002-7863/90/1512-1333$02.50/0

We find that polymer growth occurs predominantly along step sites on the basal plane of HOPG. We also find that experimental conditions reported to promote Re–Re bond formation yield an adsorbed product consistent with vinyl–vinyl coupling of two or more Re–Re bonded dimers.

Experimental Section

STM images were obtained with a Nanoscope II (Digital Instruments, Santa Barbara, CA). Images were recorded in constant current mode at scan rates of 1.0–3.5 Hz depending on the size of the area scanned. Tunneling tips were constructed from mechanically cut platinum–30% rhodium wire. Tips were tested for atomic resolution on graphite prior to imaging samples. Bias voltages and tunneling currents are listed in figure captions. Images were low-pass filtered.

$[Re(CO)_3(vbpy)Cl]$ was prepared according to the procedure of Wrighton and Morse.[14] Tetra-*n*-butylammonium perchlorate, TBAP (G. F. Smith), was recrystallized three times from ethyl acetate and dried in vacuum at 90 °C for 72 h. Spectroscopic grade acetonitrile (CH_3CN) was dried over 4 Å molecular sieves. Water was purified (18 MΩ) with a Water Prodigy apparatus (Labconco Corp.). All other reagents were of analytical grade and were used without further purification.

Electrodes were prepared with ~0.5 × 1.0 cm HOPG (Grade B, Union Carbide). The HOPG substrate was mounted perpendicular to the end of a glass tube with epoxy, exposing the front basal plane and edges to the solution. Electrical contact to the back side of the HOPG sample was made with a copper wire and a drop of mercury. Following electrodeposition of $[Re(CO)_3(vbpy)Cl]$, the electrode was rinsed with acetone and water and subsequently dried. The HOPG substrate was detached from the glass tube for STM measurements by inserting a razor blade between the substrate and the epoxy.

Electrochemical experiments were performed with a Princeton Applied Research Model 173 potentiostat and a Model 175 Universal Programmer. The electrochemical cell consisted of a sodium saturated calomel reference electrode (SSCE), a platinum foil counter electrode, and the HOPG working electrode. Solutions were purged with prepurified N_2.

Results

Voltammetry of $[Re(CO)_3(vbpy)Cl]$ on HOPG. A key point of the present work is to demonstrate that the molecular structures identified by STM can be correlated with the voltammetric behavior observed during the reductive electrodeposition of $[Re(CO)_3(vbpy)Cl]$ as well as with other existing mechanistic information.[1,5] In particular, we show that the electrode potential can be controlled during deposition so as to yield either a polymeric film or adsorbed "dimerized" products.

The cyclic voltammetric behavior of HOPG electrodes in N_2-purged CH_3CN/0.1 M TBAP containing 2 mM $[Re(CO)_3(vbpy)Cl]$ is shown in Figure 1 and is essentially identical with that observed on platinum electrodes. On the initial negative-going potential sweep (beginning at 0.0 V), a reduction wave (i_p at −1.35 V) is observed corresponding to the largely vinylbipyridine localized 1e⁻ reduction of the parent compound, eq 1. Repeated

$$Re(CO)_3(vbpy)Cl + e^- \rightleftharpoons [Re(CO)_3(vbpy)Cl]^{\bullet -} \quad (1)$$

cycling of the electrode potential to a value slightly beyond the peak of this wave (e.g., −1.45 V) results in deposition of an electroactive film, as evidenced by an increase in the voltammetric currents, Figure 1a, and the appearance of a brownish-yellow film on the electrode surface. In addition to polymerization, the radical anion can undergo chemical reaction to yield a Re–Re bonded dimer,[5] eq 2. Further electroreduction of $[Re(CO)_3(vbpy)Cl]^{\bullet -}$ to the dianion at −1.75 V results in fast chloride lost, thereby enhancing the rate of dimer formation.

$$2[Re(CO)_3(vbpy)Cl]^{\bullet -} \rightarrow [(CO)_3(vbpy)Re\text{–}Re(CO)_3(vbpy)] + 2Cl^- \quad (2)$$

On the basis of the voltammetric behavior of the dimethyl analogue,[5a] [Re(4,4′-dimethyl-2,2′-bipyridine)$(CO)_3$Cl], which also undergoes electrochemical initiated dimerization (see Scheme I in ref 5a), the second reduction wave at −1.55 V in Figure 1b (intermediate between the first and second reduction waves of the parent compound) has been assigned to the reversible 1e⁻ reduction of the dimer. The small, irreversible oxidation wave at −0.15 V

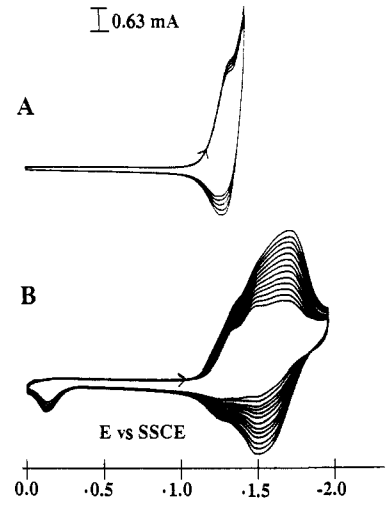

Figure 1. Cyclic voltammetric response (beginning with the third scan) of a HOPG electrode in acetonitrile containing $[Re(CO)_3(vbpy)Cl]$ and 0.1 M TBAP: (a) potential scan from 0.0 to −1.45 V vs SSCE, voltammetric sweep rate = 50 mv/s and (b) from 0.0 to −2.0 V vs SSCE. Voltammetric sweep rate = 100 mv/s.

(Figure 1b) has been assigned to the 1e⁻ oxidation of the metal–metal bond of the dimer to the corresponding radical cation.[5a]

Film growth occurs whether the potential is switched prior to or following the dimer reduction wave centered at −1.55 V, Figure 1 (parts a and b, respectively). However, previous UV–vis spectroscopy of $[Re(vbpy)(CO)_3Cl]$ based films,[1b] and the notable absence of the dimer oxidation wave at −0.15 V in Figure 1a demonstrate that films can be grown without significant inclusion of the Re–Re metal-bonded species. In the following section, we present STM images of polymer-coated HOPG electrodes prepared so as to promote or suppress the generation of Re–Re metal-bonded species in the film. Since both the front and edges of the electrode substrate were exposed to the $[Re(CO)_3(vbpy)Cl]$ solution (see Experimental Section), it was not possible to coulometrically measure the surface coverage of electroactive species deposited only on the basal plane of the HOPG.

Scanning Tunneling Microscopy. Figure 2 shows STM images of HOPG electrodes cycled between 0.0 V and −2.0 V in a CH_3CN/0.1 M TBAP solution containing 2 mM $[Re(CO)_3(vbpy)Cl]$. As described in the previous section, both polymeric and dimeric products of $[Re(CO)_3(vbpy)Cl]$ reduction are evident from the voltammetric behavior (Figure 1b) when the electrode potential is cycled between these potential limits. STM images of electrodes prepared in this way show what appear to be discrete species (i.e., nonpolymeric) uniformly distributed over large regions of the surface, Figure 2a, as well as scattered polymer aggregates (not shown in Figure 2; a latter section describes polymer morphologies found when the electrode is cycled between 0.0 and −1.45 V). Three different species were observed, Figure 2, each based on a sphere of approximately 16 Å in diameter: (i) a single sphere, (ii) pairs of spheres separated by a region 5–7 Å long, and (iii) trimers of spheres in a triangular (V-shape) arrangement. STM images show that the predominant molecular form is that corresponding to the pair of spheres.

There is some uncertainty as to whether all of the molecular entities observed in Figure 2 are in direct contact with the HOPG substrate or whether they represent the outermost layer of an adsorbed film. The surface coverage of Re sites on both edge and basal planes, as measured by integration of the voltammetric wave, is ca. 3×10^{-10} mol/cm², corresponding to a film approximately three molecular layers thick. However, the fact that the underlying structure of the HOPG could be observed at high magnification (vide infra) suggests that the species observed here are indeed in intimate contact with the graphite surface and that there is no intervening polymeric film. Attempts to image the molecules at scan sizes of approximately 150 × 150 Å or less would cause the molecules to *appear* to break apart and the graphite corrugations from the HOPG to become superimposed on the molecule, Figure

(14) Wrighton, M. S.; Morse, D. L. *J. Am. Chem. Soc.* **1974**, *96*, 988.

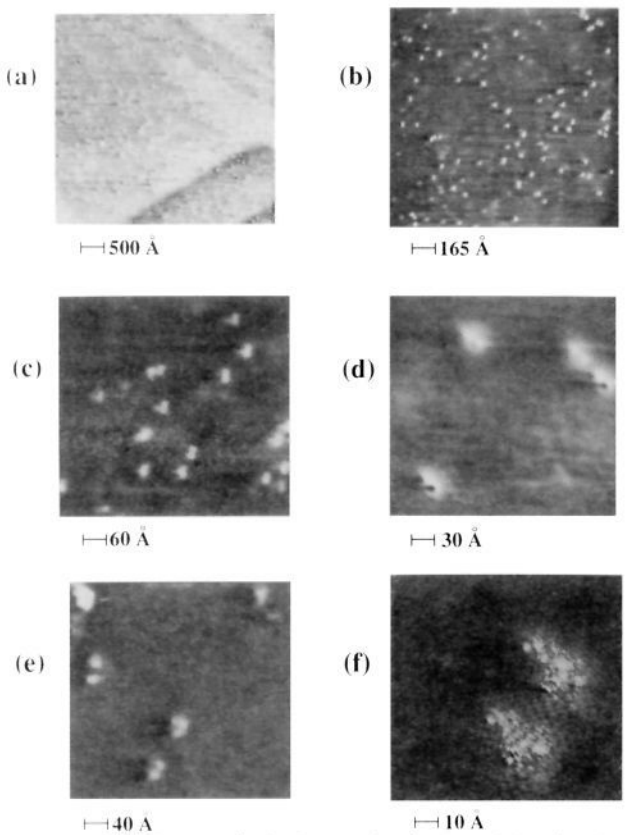

Figure 2. STM images of HOPG electrode after potential cycling between 0.0 and −2.0 V vs SSCE in acetonitrile containing 2 mM [Re(CO)$_3$(vbpy)Cl] and 0.1 M TBAP. (a) 5700 × 5700 Å image showing uniform coverage by adsorbed molecules (image recorded at bias voltage, V_t (substrate voltage with respect to tip), and setpoint current, i_t, of 0.03 V and 0.75 nA). The contrast between the darkest and lightest regions corresponds to a height, Z_{vert}, of 80 Å. (b) 1900 × 1900 Å image (V_t, i_t) = (0.165 V, 0.30 nA); Z_{vert} = 20 Å. (c) 680 × 680 Å image (V_t, i_t) = (0.165 V, 0.30 nA); Z_{vert} = 18 Å. (d) 320 × 320 Å image (V_t, i_t) = (−0.287 V, 2.3 nA); Z_{vert} = 13 Å. (e) 460 × 460 Å image (V_t, i_t) = (−0.022 V, 0.35 nA); Z_{vert} = 40 Å. (f) 110 × 110 Å image (V_t, i_t) = (−0.287 V, 2.3 nA); Z_{vert} = 27 Å.

2f. Upon increasing the scan size once again, the intact molecule would reappear at its original position. We speculate that this degradation in resolution is a result of diffusional and/or rotational motion of the molecule that may be induced by the scanning tip. Attempts to image adsorbed species prepared by evaporation of an acetonitrile solution of the [Re(CO)$_3$(vbpy)Cl] monomer or the Re–Re dimer of the dimethyl analogue, [(Re(4,4′-dimethyl-2,2′-bipyridine)(CO)$_3$)$_2$], on HOPG were unsuccessful. In both cases, only the graphite structure was apparent suggesting that rapid molecular motion on the substrate, whether tip induced or not, prevents imaging these species.

Variations in the STM images with bias voltage were also noted. Figure 2d shows images taken at a bias voltage of −286.9 mV and a tunneling current of 2.3 nA. Although the basic shape is the same as before, each lobe of the dumbbell is now approximately 13 Å in diameter, while the distance between the lobes is still 6–7 Å. In addition to the apparent size reduction, it is also noted that the lobes are better resolved. A region of decreased tunneling current near the center of each lobe is now apparent, as indicated by a depression (dark spot). Other researchers have speculated that the contrast in STM images of nonconducting organic molecules deposited on graphite may be due to perturbation of the graphite wave functions upon mixing with the molecular orbitals of the organic molecules.[15-17] For many redox active

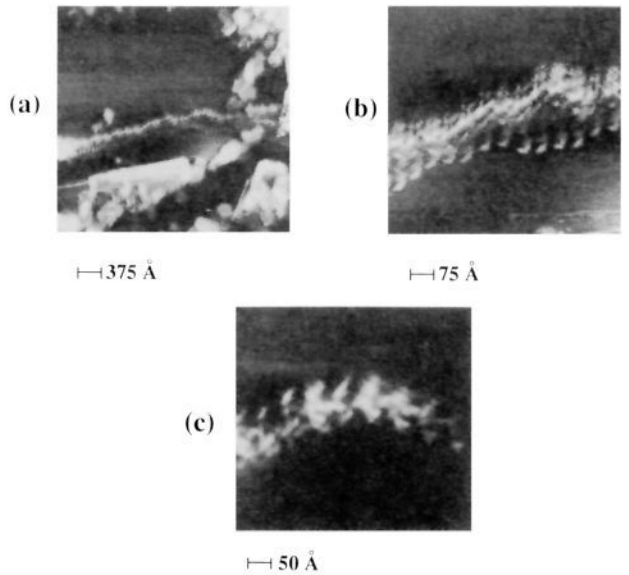

Figure 3. STM images of HOPG electrode after potential cycling between 0.0 and −1.45 V vs SSCE in acetonitrile containing 2 mM [Re(CO)$_3$(vbpy)Cl] and 0.1 M TBAP. (a) 4200 × 4200 Å image showing an isolated polymer strand 2770 Å long; Z_{vert} = 100 Å. (b) 840 × 840 Å image showing detailed structure of the polymer strand in part (a). The spheres that constitute the backbone of the strand are approximately 38 Å in diameter; Z_{vert} = 70 Å. Images in (a) and (b) were recorded at (V_t, i_t) = (0.068 V, 0.68 nA). (c) 580 × 580 Å image of the same polymer chain as in part (a) (V_t, i_t) = (0.138 V, 0.68 nA); Z_{vert} = 50 Å. The polymer chain appears to have rotated to a new position and now appears as a feather-like strand.

molecules, e.g., [Re(CO)$_3$(vbpy)Cl]-based adsorbates, the electron acceptor and donor states normally associated with electron-transfer reactions may also provide an alternative electron conduction mechanism that is bias dependent (see Discussion).

The following section describes several polymer morphologies that were well-resolved in STM imaging. First of all, it should be mentioned that no single structure described below is uniquely characteristic of the overall film. Indeed, the majority of STM images of electrodes prepared by this procedure showed large regions of bare, atomically resolved, HOPG separating other regions where poorly defined aggregates of polymer had deposited. STM observation of resolvable polymeric products required electrodeposition by cycling the potential through the first reduction wave only, Figure 1a.

A polymer strand that is about 3000 Å long is shown in the center of Figure 3a. The strand bridges the distance between aggregates of polymer material and appears to be resting along a step site on the graphite surface, as indicated by an ~8 Å height variation between the graphite regions above and below the polymer strand. Atomic resolution of the HOPG substrate was observed in the regions above and below the polymer strand.

The STM image in Figure 3b shows that the polymer appears as a strand of ~38 Å diameter spheres. Regularly spaced, shorter segments, approximately 100 Å long by 13 Å wide, appear to be linked to the main strand in the direction toward the bottom of the image. The total height of the strand above the surface is approximately 10 Å. Stable images of the polymer strand, taken at a bias voltage of 67.7 mV and a tunneling current of 0.68 nA, were observed for a period of about 2.5 h. Figure 3c shows the same polymer strand following a change in the bias voltage from 67.7 to 137.6 mV and a scan size to 600 × 600 Å. Even though the polymer length remained the same the morphology now resembled a feather-like strand. The strands protruding from the backbone were approximately 60 Å long and 20 Å wide. It is not known whether the change was induced by the altered bias voltage,

(15) Spong, J. K.; Mizes, H. A.; LaComb, L. J.; Dovek, M. M.; Frommer, J. E.; Foster, J. S. *Nature* **1989**, *338*, 137.

(16) Smith, D. P. E.; Horber, H.; Gerber, Ch.; Binnig, G. *Science* **1989**, *245*, 43.

(17) Wu, X.; Lieber, C. M. *J. Phys. Chem.* **1988**, *92*, 5556.

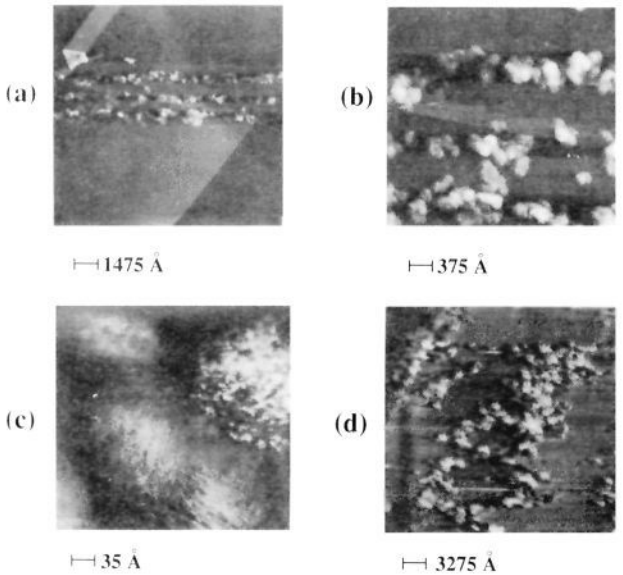

Figure 4. STM images of HOPG electrodes following same treatment as in Figure 3. (a) 17000 × 17000 Å image of polymer spheres nucleated along step sites (Z_{vert} = 120 Å). (b) 4200 × 4200 Å (Z_{vert} = 120 Å); and (c) 420 × 420 Å image (Z_{vert} = 60 Å) of same region as in part (a). Images in (a)–(c) were recorded at (V_t, i_t) = (0.05 V, 0.68 nA). (d) 38000 × 38000 Å image of a different HOPG electrode showing crown-type polymer morphology, (V_t, i_t) = (0.03 V, 30 nA); Z_{vert} = 300 Å.

a tip-induced rotation upon changing the scan size, or whether the tip itself had changed.

Various polymer morphologies were observed on the same electrode. Figure 4a,b shows spherically shaped (200–300 Å diameter) polymeric deposits along several step sites on the surface. No deposits were observed on the substrate in regions removed from the steps. STM images of the spheres taken at higher magnification show that they appear to be composed of fibrils ca. 8–10 Å in diameter, Figure 4c. Prolonged STM scanning tended to dislodge the spheres.

Figure 4d shows a different polymer morphology with a shape which can be likened to a "crown-type" structure with the crowns coalescing to form larger domains. The base area of the crown is ca. 10^6–10^7 Å^2 with segments extending upward from the surface to a height of ca 75–125 Å. Polymer growth is observed at step sites (see left-hand corner image) as well as on apparently flat regions of the substrate.

Discussion

Interpretation of the STM images of products derived from electroreduction of $[Re(CO)_3(vbpy)Cl]$ requires consideration of two primary observations. First, the structures of adsorbed products (polymer vs discrete aggregates) are markedly dependent on the potential range employed in the electrodeposition. This observation suggests that at least two distinct chemical mechanisms lead to adsorbed products. The second observation that we focus on is the size and shape of the uniformly distributed molecules observed when the potential is cycled to potentials to promote Re–Re bond formation.

We begin by considering the potential dependence of the deposited structures. As mentioned previously, deposition of polymeric products was enhanced when the potential scan was between 0.0 and −1.45 V. On the other hand, the formation of discrete species (nonpolymeric aggregates) was greatly enhanced over polymer deposition when the potential was scanned between 0.0 and −2.0 V. These observations can be understood in terms of the relative rates of dimerization (or formation of larger yet discrete species) versus polymerization.

As mentioned previously, the first reduction process for $[Re(CO)_3(vbpy)Cl]$ is a largely ligand-localized process giving the radical anion which in a subsequent slow step can loose chloride and dimerize to $[Re(CO)_3(vbpy)_2]$. Mechanistically, this process likely involves a (slow) partial intramolecular electron transfer to a metal-localized dσ* orbital (strongly antibonding) resulting in chloride loss and subsequent dimerization. Further reduction of the radical anion (at about −1.75 V) to the dianion results in extremely fast chloride loss since the electron goes directly into a metal based dσ* orbital.[5a]

Scheme I

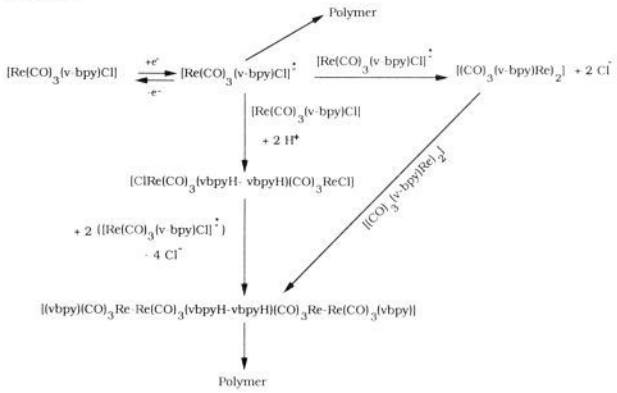

In competition with these processes is polymer formation which could, in principle, occur by (a) linear vinyl–vinyl coupling or by (b) radical–radical coupling between the vinyl substituent and a carbon atom of the vbpy ring system. Because of severe steric constraints, it is unlikely that linear vinyl–vinyl coupling can account for polymer growth. This has been inferred from studies on related complexes of Fe, Ru, and Os where the number of vinyl groups in the complex was varied from one to three.[2] Part of this steric strain could be relieved by having a propagation mechanism involving radical–radical coupling between the vinyl substituent and a carbon atom of the vbpy ligand. The existence and importance of such a pathway was unequivocally demonstrated by Guarr and Anson.[4]

In light of these facts, we can consider the potential dependent structures observed in this work. Scheme I pictorially depicts the various electrochemical and chemical steps involved. Cycling the electrode potential between 0.0 and −1.45 V generates only the anion radical which will slowly loose chloride and dimerize. However, since the electron resides primarily in a ligand-based orbital which is responsible for polymerization and since chloride loss is slow, we are in effect favoring the rate of polymerization vs that of dimerization.

On the other hand, when the potential is scanned out to −2.0 V, the generated dianion can rapidly loose chloride and dimerize. Such dimeric (or higher aggregates) species will experience even more severe steric constraints for polymerization compared to the monomeric species. Thus, in this potential regime we, in effect, accelerate the dimerization (or other aggregation) pathway over polymer formation.

The size and shape of the adsorbed discrete products observed in the STM images, Figure 2c–e, are inconsistent with the formation of single Re–Re bonded dimers. Analysis of the images indicates that each lobe of the dumbbell is ca. 16 Å in diameter, considerably larger than the size of one Re monomer. The separation distance between the edge of the lobes is ca. 6–7 Å, which is considerably larger than the Re–Re bond distance which for $[(CO)_5Re]_2$ has been determined to be 3.02 Å and represents an upper limit.[18] The total height of the dumbbells above the HOPG surface is 6–10 Å. On the basis of size considerations we propose that this entity is a tetrameric species, with each lobe of the dumbbell composed of two $Re(CO)_3(vbpy)$ units joined through a Re–Re metal bond, and the coalescence of two such species is via vinyl–vinyl coupling, Scheme I. The dimensions reported above for the observed entities, however, may differ slightly from the true molecular dimensions, since STM images electronic states of the sample rather than actual physical topography.

(18) Dahl, L. F.; Ishishi, E.; Rundle, R. E. *J. Chem. Phys.* **1957**, *26*, 1750.

It is interesting to note that polymer electrodeposition at potentials below -1.45 V is quite sensitive to the structural details of the electrode substrate. Figures 3 and 4a-c show examples of polymer deposited along step sites that are exposed on the otherwise atomically smooth basal plane of HOPG. These results demonstrate that defects provide a significantly larger number of sites conducive to polymer nucleation leading to stable polymer deposits. Consequently, STM images of the $[Re(CO)_3(vbpy)Cl]$-based polymers reflect not only the molecular details of the polymer but also the structure of the underlying substrate. For example, the polymer strand in Figure 3 follows the contour of an 8 Å high step. In this instance, multiple points of attachment must occur, since the structural correlation between the step and the polymer extends over a distance of 3000 Å. We point out that preferential nucleation at step sites on HOPG is not always observed. For example, polymer is clearly absent from the step site observed at the bottom of Figure 3b.

As a final note, the ability to image large polymeric structures, such as the 200-300 Å spherical aggregates shown in Figure 4, requires comment since direct tunneling between the STM tip and the HOPG surface over such a distance is unreasonable. We speculate that electron conduction within the interior of the polymer is supported by diffusional or migrational electron transport via a redox conduction mechanism.[19] Dry films of partially oxidized or reduced redox polymers, e.g., poly(vinylferrocene)$^{0/+}$, when sandwiched between two macroscopic metal contacts (i.e., metal/polymer/metal) conduct electrons at a rate controlled by electron hopping between oxidized and reduced sites.[20,21] These solid-state polymer-based electrochemical cells, in fact, closely resemble the Pt-Rh tip/polymer/HOPG structure that is engaged in STM imaging of the electrodeposited $[Re(CO)_3(vbpy)Cl]$-based polymer.

(19) Murray, R. W. *Electroanalytical Chemistry*; Bard, A. J., Ed.; Wiley: New York, 1984; Vol. 14, and references therein.
(20) Jerigan, J. C.; Chidsey, C. E. D.; Murray, R. W. *J. Am. Chem. Soc.* **1985**, *107*, 2824.
(21) Hagemeister, M. P.; White, H. S. *J. Phys. Chem.* **1987**, *91*, 150.

Conclusions

STM results reported here demonstrate that the chemical composition and structure of $[Re(CO)_3(vbpy)Cl]$-based films are remarkably dependent on conditions employed in electrodeposition. Polymeric materials with several different morphologies are observed when the deposition is carried out to -1.45 V vs SSCE. A more uniform surface coverage of discrete molecules is observed when the potential is scanned to -2.0 V to promote the formation of the Re-Re dimers. On the basis of the size and shape of these entities, we tentatively assign them as products derived from vinyl-vinyl coupling of Re-Re bonded dimers: $[(vbpy)(CO)_3Re\text{-}Re(CO)_3(vbpyH\text{-}vbpyH)(CO)_3Re\text{-}Re(CO)_3(vbpy)]$.

The ability to resolve individual molecules as well as the molecular subunits in the $[Re(CO)_3(vbpy)Cl]$-based polymer suggest that STM studies may be valuable in identifying the structure of surface-adsorbed organometallic species. In addition, the substitutional chemistry of $[Re(CO)_3(vbpy)Cl]$ and other similar metal complexes containing polymerizable ligands is significant thus broadening the range of applications. We are currently exploring these and other areas.

Acknowledgment. STM facilitates are supported by the Center for Interfacial Engineering with funding from NSF Engineering Research Centers Program (CDR 8721551) and industrial sponsors. Work at the University of Minnesota is supported by the Office of Naval Research Young Investigator Program. Work at Cornell was supported in part by the National Science Foundation. S.L. acknowledges support by a MARC Fellowship from the NIH. H.D.A. is the recipient of a Presidential Young Investigator Award (1984-1989) and an A. P. Sloan Fellowship (1987-1991).

Electrochemistry of NADH/NAD$^+$ Analogues. A Detailed Mechanistic Kinetic and Thermodynamic Analysis of the 10-Methylacridan/10-Methylacridinium Couple in Acetonitrile

Philippe Hapiot,[1a] Jacques Moiroux,[1b] and Jean-Michel Savéant*,[1a]

Contribution from the Laboratoire d'Electrochimie Moléculaire de l'Université de Paris 7, Unité de Recherche Associée au CNRS No. 438, 2, Place Jussieu, 75231 Paris Cedex 05, France, and the Laboratoire de Chimie Analytique, Université de Paris 5, Unité de Recherche Associée No. 484, 4, Avenue de l'Observatoire, 75270 Paris Cedex 05, France. *Received July 7, 1989*

Abstract: The electrochemical oxidation of 10-methylacridan (AH) at platinum and gold electrodes in acetonitrile containing various pyridine bases is investigated by means of cyclic voltammetric and potential step techniques. The conversion of AH to the 10-methylacridinium ion (A^+) proceeds along an electron-proton-electron transfer mechanism, the second electron being abstracted by the initial cation radical, $AH^{\bullet+}$, rather than by the electrode itself in most cases. The use of ultramicroelectrodes (in the 10 μm diameter range) allows the determination of the standard potential of the $AH^{\bullet+}/AH$ couple and of the rate constant of the deprotonation of $AH^{\bullet+}$; the latter was measured as a function of the pK_a of a series of pyridine bases. Investigation of the reduction of A^+ by the same techniques led to the determination of the standard potential of the $A^+/A^\bullet$ couple and of the dimerization rate constant of $A^\bullet$. The oxidation of AH as well as the reduction of A^+ are kinetically controlled by follow-up homogeneous chemical steps rather than by the initial electron transfer, which appears as quite fast in both cases. The combination of an ultraslow spectrometric technique with the ultrafast electrochemical techniques allowed the determination of the pK_a of the $AH^{\bullet+}/A^\bullet$ couple from that of the standard potential of the overall reaction $AH \rightleftharpoons A^+ + 2e^- + H^+$ and hence the construction of a Brønsted plot with a known driving force origin for the deprotonation of $AH^{\bullet+}$.

The mechanism of the conversion of NADH to NAD$^+$ and of the reverse reaction, in the coenzyme itself as well as in synthetic analogues, has been the object of considerable experimental work and discussion during the last 15 years.[2] The issue of whether

0002-7863/90/1512-1337$02.50/0